


Opiate dependence induces cell type-specific plasticity of intrinsic membrane properties in the rat juxtacapsular bed nucleus of stria terminalis (jcBNST)

Walter Francesconi^{1,2} · Attila Szücs^{3,4} · Fulvia Berton^{2,5} · George F. Koob^{6,7} · Leandro F. Vendruscolo^{6,8} · Pietro Paolo Sanna⁹ 

Received: 2 May 2017 / Accepted: 5 September 2017 / Published online: 6 October 2017
© Springer-Verlag GmbH Germany 2017

Abstract

Rationale Drugs of abuse can alter circuit dynamics by modifying synaptic efficacy and/or the intrinsic membrane properties of neurons. The juxtacapsular subdivision of the bed nucleus of stria terminalis (jcBNST) has unique connectivity that positions it to integrate cortical and amygdala inputs and provide feed-forward inhibition to the central nucleus of the amygdala (CeA), among other regions. In this study, we investigated changes in the synaptic and intrinsic properties of neurons in the rat jcBNST during protracted withdrawal from morphine dependence using a combination of conventional

electrophysiological methods and the dynamic clamp technique.

Results A history of opiate dependence induced a form of cell type-specific plasticity characterized by reduced inward rectification associated with more depolarized resting membrane potentials and increased membrane resistance. This cell type also showed a lower rheobase when stimulated with direct current (DC) pulses as well as a decreased firing threshold under simulated synaptic bombardment with the dynamic clamp. Morphine dependence also decreased excitatory postsynaptic potential amplification, suggesting the downregulation of the persistent Na⁺ current (I_{NaP}).

Conclusion These findings show that a history of morphine dependence leads to persistent cell type-specific plasticity of the passive membrane properties of a jcBNST neuronal population, leading to an overall increased excitability of such neurons. By altering the activity of extended amygdala circuits where they are embedded, changes in the integration properties of jcBNST neurons may contribute to emotional dysregulation associated with drug dependence and withdrawal.

Walter Francesconi and Attila Szücs contributed equally.

✉ Pietro Paolo Sanna
psanna@scripps.edu

¹ Department of Molecular Medicine, The Scripps Research Institute, La Jolla, CA, USA

² Department of Anatomy and Cell Biology, School of Medicine, University of Illinois at Chicago, Chicago, IL, USA

³ BioCircuits Institute, University of California San Diego, La Jolla, CA, USA

⁴ MTA-ELTE NAP-B Neuronal Cell Biology Group, Eötvös Lóránd University, Budapest, Hungary

⁵ Dipartimento di Biologia, Università degli Studi di Pisa, Pisa, Italy

⁶ Department of Neuroscience, The Scripps Research Institute, La Jolla, CA, USA

⁷ National Institute on Alcohol Abuse and Alcoholism, National Institutes of Health, Rockville, MD, USA

⁸ National Institute on Drug Abuse, National Institutes of Health, Baltimore, MD, USA

⁹ Department of Immunology and Microbiology and Department of Neuroscience, The Scripps Research Institute, La Jolla, CA, USA

Keywords Opiates · Physiological properties · Synaptic integration · Dynamic clamp

Abbreviations

BLA	Basolateral nucleus of amygdala
BNST	Bed nucleus of stria terminalis
sEPSC	Spontaneous excitatory postsynaptic current
EPSP	Excitatory postsynaptic potential
I_{KIR}	Inward-rectifying K ⁺ current
I_{NaP}	Persistent Na ⁺ current

Introduction

The bed nucleus of the stria terminalis (BNST) is involved in coordinating autonomic responses, the effects of drugs of abuse and stress, and the affective components of pain (Aston-Jones et al. 1999; Aston-Jones and Harris 2004; Epping-Jordan et al. 1998; Francesconi et al. 2009; Ren et al. 2009; Silberman and Winder 2013; Stamatakis et al. 2014; Tran et al. 2014).

The juxtacapsular nucleus (jcBNST) is located in the dorsolateral portion of the BNST (Dong et al. 2000; Larriva-Sahd 2004), and the target of excitatory projections from the basolateral nucleus of the amygdala (BLA) and inputs from the dysgranular insular cortex and infralimbic cortex (Dong et al. 2001; Larriva-Sahd 2004; McDonald et al. 1999; Shammah-Lagnado and Santiago 1999). In turn, the jcBNST sends a dense, mostly or exclusively γ -aminobutyric acid (GABA)-ergic, projection to the medial central nucleus of the amygdala (CeA), the main output nucleus of the amygdala (Dong et al. 2001; Larriva-Sahd 2004). The jcBNST also provides inputs to the ventromedial caudoputamen, anterior basolateral amygdalar nucleus, caudal substantia innominata, a caudal dorsolateral region of the substantia nigra, mesencephalic reticular nucleus, and retrorubral area as well as light inputs to the prelimbic, infralimbic, and ventral CA1 cortical areas; to the posterior basolateral, posterior basomedial, and lateral amygdalar nuclei; to the paraventricular and medial mediodorsal thalamic nuclei; to the subthalamic and parasubthalamic nuclei of the hypothalamus; and to the ventrolateral periaqueductal gray (Dong et al. 2001; Larriva-Sahd 2004). The connectivity of the jcBNST in rodents and primates appears to be largely consistent (deCampo and Fudge 2013).

The jcBNST is unique because it is the only lateral BNST component that does not receive GABAergic inputs from the CeA (Dong et al. 2001; Larriva-Sahd 2004). Thus, the jcBNST is well positioned within extended amygdala circuits to integrate limbic and cortical inputs and contribute to the modulation of the CeA output (Francesconi et al. 2009; Francesconi et al. 2009). Therefore, changes in the integration properties of jcBNST neurons can contribute to the emotional dysregulation associated with drug dependence and withdrawal (Epping-Jordan et al. 1998; Francesconi et al. 2009; Francesconi et al. 2009; Koob and Volkow 2010).

Opioid abuse remains a considerable societal problem (SAMHSA 2013). The number of people with opioid dependence or abuse in 2012 was approximately twice the number in 2002 (SAMHSA 2013). In addition to illicit opioids, the abuse of prescription opioids or nonmedical prescription opioid use has significantly increased in the last decade and been responsible for considerable rates of morbidity, hospital admissions, and mortality (Frenk et al. 2015; Shurman et al. 2010). The increase in nonmedical prescription opioid use

parallels a considerable increase in the rates of opioid analgesic prescriptions by physicians, primarily for chronic pain conditions (Goldner et al. 2014). Understanding the cellular and circuit bases for the long-lasting functional changes induced by a history of opioid dependence is key to identifying the factors that contribute to the susceptibility to addiction and relapse after cessation. In particular, protracted dysregulation of the brain reward and stress systems, involving impaired reward function and sensitization of stress system circuitry that persists long after symptoms of acute withdrawal subside, are likely to contribute to long-lasting vulnerability to relapse after the cessation of drug taking (Diana et al. 1999; Francesconi et al. 2009; Harris and Aston-Jones 2007; Shurman et al. 2010; Stinus et al. 2000).

Here, we investigated the intrinsic membrane properties and synaptic responses of jcBNST neurons during protracted withdrawal from morphine dependence in rats. In addition to conventional electrophysiological techniques, we employed the dynamic clamp technique to study the firing responses and excitability of jcBNST neurons (Szucs et al. 2010). A history of opiate dependence induced a form of cell type-specific plasticity of intrinsic membrane properties characterized by a reduction of the inward rectification, depolarization of the resting membrane potential and increased membrane resistance, suggestive of downregulation of the inward-rectifying K^+ current (I_{KIR}). This cell type also showed a lower rheobase when stimulated with DC pulses as well as a decreased firing threshold under simulated synaptic bombardment with the dynamic clamp. Morphine dependence also decreased excitatory postsynaptic potential amplification, suggesting the downregulation of the persistent Na^+ current (I_{NaP}), whereas miniature excitatory postsynaptic currents were unaltered.

These findings support the hypothesis that alterations of the intrinsic cellular properties and excitability of specific neurons in the extended amygdala induced by a history of drug dependence mediate long-term functional changes in extended amygdala circuits during protracted abstinence.

Materials and methods

Ethical standards

All of the animal protocols were consistent with the guidelines issued by the National Institutes of Health and approved by the Institutional Animal Care and Use Committee of The Scripps Research Institute.

Chronic morphine treatment

To induce dependence, rats were implanted with morphine pellets that were provided by the National Institute on Drug

Abuse. Two morphine pellets (75 mg morphine base each) were subcutaneously implanted in the rat's back under isoflurane anesthesia. Control rats were implanted with placebo pellets. After 10 days of placebo or morphine exposure, the pellets were removed under isoflurane anesthesia so that the rats were no longer exposed to morphine and would go through withdrawal. The rats were euthanized 10–15 days after withdrawal for acute brain slice preparation for electrophysiological recordings.

Mechanical sensitivity testing

For mechanical hypersensitivity testing, separate rats were placed in individual plastic compartments (26 × 11 × 20 cm) with stainless steel mesh floors for 30 min until the rats' grooming and exploratory behaviors ceased. To assess the presence of mechanical hypersensitivity, the mid-plantar area of each hindpaw was perpendicularly stimulated with calibrated nylon von Frey filaments (Weinstein–Semmes algesiometer forces) for 5 s using the up-down method, starting with the 28.84-g force. A brisk withdrawal of the paw was considered a positive response. Paw withdrawal thresholds were measured 10 days after the end of morphine exposure, corresponding with the time of electrophysiological recordings.

Brain slice preparation

Acute brain slices were prepared as previously described (Francesconi et al. 2009) with minor modifications. Briefly, coronal rat brain slices (350 μm) were collected from the rostral cerebrum of Wistar rats using a Leica vibrating microtome (Wetzlar, Germany: Pathology Leaders) in oxygenated artificial cerebrospinal fluid (aCSF), consisting of 130 mM NaCl, 3.5 mM KCl, 24 mM NaHCO₃, 1.25 mM NaH₂PO₄, 2.2 mM CaCl₂, 10 mM D-glucose, and 2 mM MgSO₄, pH 7.4. The slices were preincubated in aCSF for 1 h at 32 °C and then maintained at room temperature for at least 30 min before being transferred to a submerged recording chamber. The temperature of the aCSF in the recording chamber was kept at 31 °C during the recordings, and the perfusion was run at 3 ml/min. Slices of brain tissue that contained the jcBNST were placed in a superfusion chamber and visualized with a Leica stereomicroscope under low magnification. Neurons were not visualized during electrode insertion or the experiments (blind patching). Intracellular current clamp and dynamic clamp experiments were performed in whole-cell configuration using 8–12 MΩ patch pipettes filled with intracellular solution that contained 120 mM K gluconate, 10 mM KCl, 3 mM MgCl₂, 10 mM HEPES, 10 mM phosphocreatine, 2 mM MgATP, and 0.2 mM guanosine triphosphate; osmolarity was set to 280–290 mOsm, pH 7.2. The synaptic isolation of jcBNST neurons was achieved by blocking glutamate and

GABA receptors using 10 μM 6-cyano-7-nitroquinoxaline-2,3-dione (CNQX), 50 μM AP-5, and 30 μM bicuculline in the bath.

Whole-cell patch clamp and intracellular stimulation

Recordings and intracellular stimulation were performed using a Multiclamp 700 amplifier (Axon Instruments). Stimulus waveforms were generated using the data acquisition software DASYLab 11.0 (National Instruments) on a Windows computer equipped with a National Instruments PCI-MIO-16-E4 board. Standard rectangular current commands were used as stimuli for the initial physiological characterization of jcBNST neurons. Specifically, 350 ms pulses of current were delivered starting from –200 pA and increased at increments of 5 or 10 pA (a 0 pA holding current was used throughout the experiments). The voltage responses of jcBNST neurons were analyzed using our custom software (IV Analyzer, Szucs et al. 2012). A total of six physiological parameters were extracted from the voltage responses of the neurons, including resting membrane potential, input resistance, voltage sag, and input-output gain (Table 1). Miniature excitatory postsynaptic currents (mEPSCs) were recorded in voltage-clamp mode at –70 mV holding potential. The arrival time of mEPSC events was determined by local evaluation of the statistical properties of the current waveform.

Dynamic clamp and simulated synaptic inputs

In addition to the conventional current clamp stimulation, the firing activity of jcBNST neurons was elicited by stimulating them with simulated excitatory and inhibitory synaptic inputs via dynamic clamp (Nowotny et al. 2006). This allowed the evaluation of the excitability of jcBNST neurons under the action of sparse simulated synaptic inputs or more intense bombardment. The simulated synaptic inputs were generated by coupling computer-generated voltage waveforms (serving as presynaptic voltage) to the dynamic clamp system and using the membrane potential of the biological neuron as postsynaptic voltage. Two types of template waveforms were used: (A) separate EPSPs at 4 Hz frequency and (B) moderate intensity bombardment at 30 Hz (mean rate). The excitability profiles (input-output relationships) of jcBNST neurons were obtained by gradually increasing the level of excitatory synaptic conductance in the successive stimulus sweeps as in our previous study (Szucs et al. 2010). Neurons at low synaptic conductance levels remained subthreshold, emitting an increasing number of spikes as the synaptic conductance increased. Input-output functions in each of the three jcBNST neuronal cell types with conventional square DC pulse injection are operationally referred to here as “static

Table 1 Physiological properties of BNST neurons

	V_{rest} [mV]	R_{rest} [M Ω]	R_{hyp} [M Ω]	Sag slope [mV/nA]	Rheobase [pA]	I-O gain [spike/nA]	Observations
Type I	-61.2 ± 1.5	377.7 ± 33.8	230.0 ± 30.7	-56.2 ± 5.2	47.9 ± 5.6	47.0 ± 7.2	Control ($n = 9$)
	-59.4 ± 1.9	523.9 ± 63.4	254.1 ± 25.4	-43.8 ± 7.6	33.6 ± 7.2	65.5 ± 12.6	Dep. ($n = 11$)
Type II	-59.1 ± 0.4	410.6 ± 33.0	280.2 ± 27.4	-67.7 ± 12.8	25.1 ± 5.9	64.0 ± 16.1	Control ($n = 6$)
	-57.6 ± 0.9	511.6 ± 43.9	312.5 ± 24.4	-53.0 ± 7.6	31.6 ± 5.9	65.5 ± 9.8	Dep. ($n = 16$)
Type III	-73.3 ± 1.0	262.4 ± 20.7	104.4 ± 5.7	N/A	91.7 ± 9.3	115.3 ± 10.3	Control ($n = 34$)
	-70.1 ± 0.9	333.0 ± 29.8	132.7 ± 9.1		68.7 ± 6.6	91.0 ± 10.5	Dep. ($n = 31$)

For each cell type, parameters are listed as measured from control animals (top) and dependent animals (bottom). Significant group differences are indicated with bold italic numbers ($p < 0.05$ level). Parameters are as follows: V_{rest} , resting membrane potential; R_{rest} , inputs resistance at rest ($I = 0$); R_{hyp} , membrane resistance measured at -200 pA current level; Sag slope, the slope of the voltage sag versus input current curve; I-O gain, the slope of the input-output relationship

excitability,” whereas excitability measures that were obtained with stochastic synaptic stimulation with the dynamic clamp are operationally referred to as “dynamic excitability.” The synthetic presynaptic voltage waveforms, injected synaptic current, and voltage output of the biological neuron were acquired simultaneously at a 20-kHz sampling rate. The presynaptic voltage waveforms (as analog output) were generated, and the response of jcBNST neurons was recorded by the DASyLab 11.0 program (National Instruments). The dynamic clamp software (StdpC) was run on a separate computer equipped with a National Instruments board (NI PCI-6289).

Results

Hyperalgesia in protracted abstinence

The method for dependence induction used is a reliable and extensively validated method that has been used to measure both spontaneous and antagonist-precipitated withdrawal (Carrera et al. 1999; Gold et al. 1994; Yoburn et al. 1985). This treatment induces dependence as demonstrated by naloxone-precipitated physical withdrawal as well as increased motivation for opiate self-administration under a progressive-ratio schedule of reinforcement (Carrera et al. 1999). Hyperalgesia can be intimately associated with the transition to drug dependence by facilitating negative reinforcement processes (Angst and Clark 2006; Edwards et al. 2012; Shurman et al. 2010; Simonnet and Rivat 2003). Thus, to investigate the presence of protracted effects of opioid dependence, separate rats were tested for mechanical hypersensitivity at 10–15 days post-withdrawal at the same time of the electrophysiological recording. We found that rats with a history of morphine dependence exhibited reduced paw withdrawal thresholds, an index of mechanical hypersensitivity, compared with control placebo-exposed rats ($t_{14} = 2.32$, $p < 0.05$), indicating that opioid dependence results in long-lasting functional changes (Fig. 1).

Characterization of jcBNST neurons

Based on their characteristic voltage responses when stimulated with hyperpolarizing and depolarizing current pulses, three types of neurons were identified in the juxtacapsular BNST (Hammack et al. 2007; Hazra et al. 2011; Szucs et al. 2010), (Table 1). In particular, type I neurons display moderate voltage sag during hyperpolarization that indicates the presence of the hyperpolarization-activated cation current (I_h) in those neurons. As a distinguishing feature of type II neurons, post-inhibitory spikes are produced in response to preceding negative current steps that are related to the action of the low-threshold Ca^{2+} current. Additionally, type II neurons display strong voltage sags under hyperpolarizing current pulses that indicate a high level of I_h in such neurons. Type III neurons differ from the previous two types in several aspects: they exhibit high rheobase and no voltage sag under negative current steps; they display prominent inward rectification that is caused by the activation of the inward-rectifying K^+ current (I_{KIR}) at membrane potentials more negative than approximately -50 mV and start firing after a characteristic slow

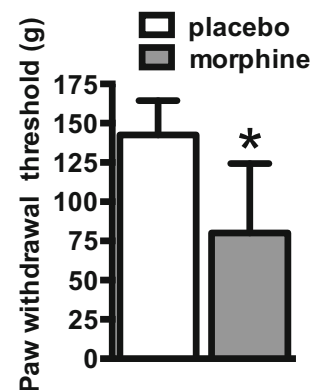


Fig. 1 Mechanical sensitivity responsiveness during protracted withdrawal in rats with a history of morphine dependence. Paw withdrawal thresholds in morphine-exposed rats were significantly lower than the ones in the control group, indicating protracted mechanical hypersensitivity in rats with histories of morphine dependence. * $p < 0.05$, significant group effect. $n = 8$ per group

voltage ramp. The above features of the voltage responses allowed us to differentiate among phenotypes of jcBNST neurons and analyze the effects of morphine withdrawal on specific membrane properties of three physiologically different groups of cells of this brain region.

Inward rectification of type III jcBNST neurons is reduced by morphine dependence

Our first objective was to determine whether protracted withdrawal in morphine-dependent animals induces neuroadaptive changes in the intrinsic membrane properties of jcBNST neurons and whether such effects are cell type-specific. A total of six physiological features (Table 1) were extracted from the voltage responses of jcBNST neurons under current step stimulation (Szucs et al. 2012). We observed a reduction of the inward rectification that characterizes type III neurons, which was associated with a depolarization of the resting membrane potential and increased membrane resistance in these neurons (Fig. 2, Table 1). The membrane resistance of type III jcBNST neurons at -200 pA test levels was significantly increased relative to neurons from control rats (Fig. 2i; 157.1 ± 10.8 vs. 118.7 ± 9.3 M Ω , $n = 33$ vs. $n = 21$, respectively, $p = 0.01$). It is important to note that the activation of inward-rectifying K current is maximal at deep hyperpolarized membrane potentials such as when using -200 pA current injections. Additionally, type III neurons exhibit no hyperpolarization-activated membrane currents other than I_{KIR} ; hence, the observed membrane resistance at this voltage regime is predominantly a manifestation of the level of I_{KIR} in these neurons. The membrane resistance was plotted as a function of the input current level, then the extrapolated membrane resistance was calculated at rest ($I = 0$) and at a -200 pA test level. Next, the linear part of the resistance curve was fitted (Fig. 2c, d). This procedure allowed an accurate assessment of the degree of inward rectification caused by the action of the inwardly-rectifying K⁺ current (I_{KIR}). The membrane resistance of type III jcBNST neurons at -200 pA test levels was significantly increased relative to neurons from control rats (Fig. 2i; 132.7 ± 9.1 vs. 104.4 ± 5.7 M Ω , $n = 31$ vs. $n = 34$, respectively, $p = 0.01$). An increase in the extrapolated membrane resistance at rest (333.0 ± 29.8 vs. 262.4 ± 20.7 M Ω , $n = 31$ vs. $n = 34$, $p = 0.05$; Fig. 2h) was also observed. The average resting membrane potential of type III neurons was significantly more depolarized in dependent rats than in control animals (-70.1 ± 0.9 vs. -73.3 ± 1.0 mV; $n = 31$ vs. $n = 34$, $p = 0.03$; Fig. 2g), consistent with the contribution of I_{KIR} to the resting membrane potential of type III neurons in the BNST (Hammack et al. 2007). In addition to the increase of membrane resistance and depolarization of the resting membrane potential of type III neurons from dependent animals, their mean rheobase was reduced (68.7 ± 6.6 vs. 97.7 ± 9.3 pA, $n = 31$ vs. $n = 34$, $p = 0.05$; Fig. 2j). Lastly, the slope of the

spike number vs. current function (I-O gain) was not significantly changed in type III neurons of dependent rats (Table 1).

With regard to the physiological properties of type I and II neurons, no significant differences were found between the control and morphine-dependent groups. The slope of the voltage sag curve in type I and II cells, which is a function of the magnitude of I_h that is expressed in these cells (Szucs et al. 2010), was unaffected by morphine dependence. Values of the physiological parameters measured are listed in Table 1.

In conclusion, analysis of the physiological parameters of jcBNST neurons in rats with a history of morphine dependence showed that type III neurons have reduced inward rectification associated with more depolarized resting membrane potentials and increased membrane resistance. This suggests that the intrinsic membrane properties of this specific cell type and, in particular, its I_{KIR} , are modified by a history of morphine dependence.

Excitability of type III neurons under simulated synaptic bombardment in dynamic clamp experiments is increased by morphine dependence

We next explored if reduction of inward rectification observed in the current step experiments might result in more intense firing in vivo in type III neurons under the action of excitatory synaptic inputs, such as the ones that arrive from glutamatergic afferents to the jcBNST from the BLA and the cortex (Francesconi et al. 2009), using the dynamic clamp to simulate synaptic bombardment (Szucs et al. 2010; Szucs et al. 2012). This hypothesis is supported by the fact that a decrease in the magnitude of the intrinsic K_{ir} current effectively increases the membrane resistance and shifts the resting membrane potential toward a more depolarized level. To test this hypothesis, we stimulated jcBNST neurons via simulated synaptic inputs under dynamic clamp conditions (Nowotny et al. 2006; Szucs et al. 2010). The design of these experiments and the neurons' firing responses are shown in Fig. 3. We generated two types of synaptic input patterns that were used to stimulate the neurons in a sequential manner. The first input pattern consisted of discrete EPSCs separated by 250 ms intervals. The second pattern simulates moderate-frequency (30 Hz) synaptic bombardment by mixing variable amplitude EPSCs and IPSCs. In each cycle of stimulation, two patterns of synaptic inputs were presented, and the strength of the input (synaptic conductance) was gradually increased to elicit firing. This protocol simulates a gradual upscaling of excitatory synaptic inputs to jcBNST neurons and parallels the protocol used under conventional current step stimulation by increasing levels of DC pulses.

For both types of input pattern, we determined the minimal level of excitatory synaptic conductance that was sufficient to evoke firing as a measure of the dynamic excitability of jcBNST neurons, paralleling the rheobase assessed

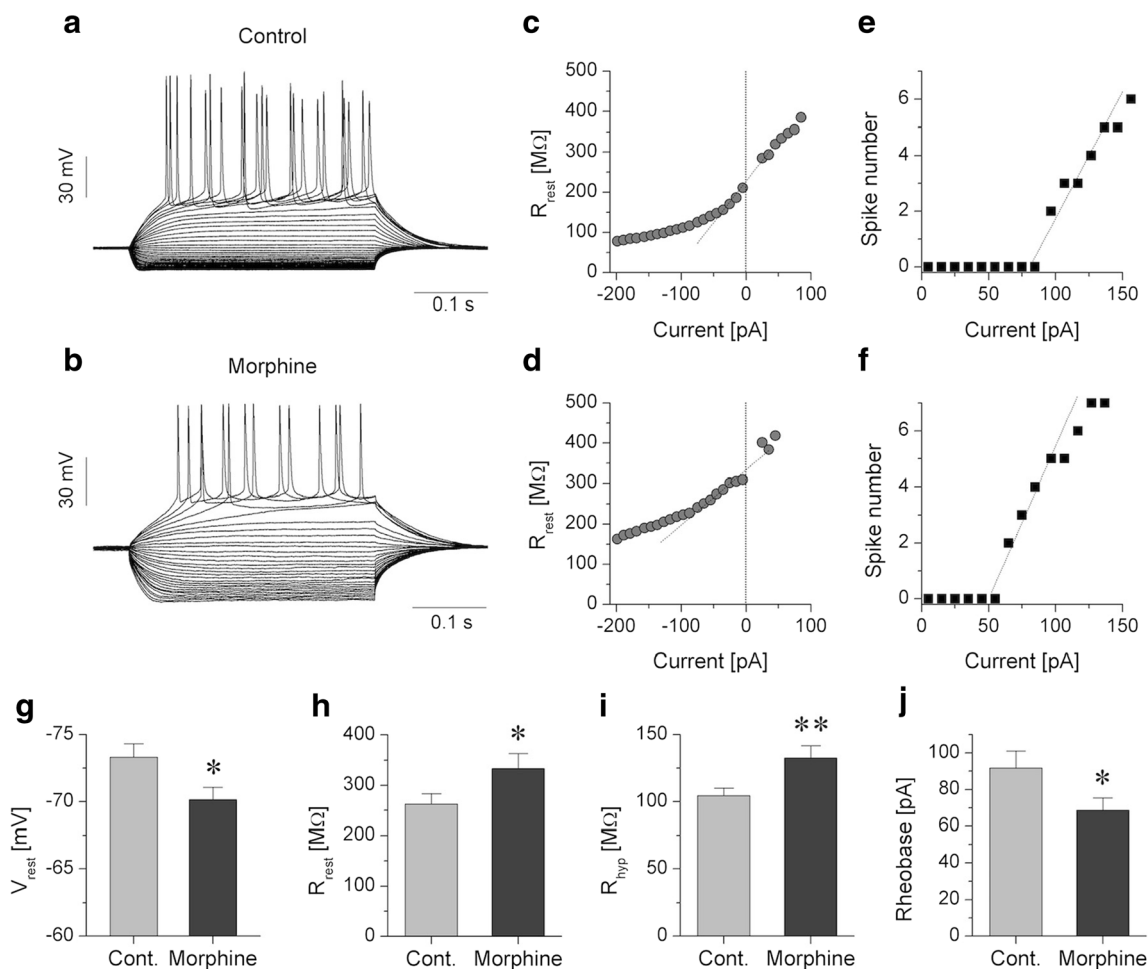


Fig. 2 Reduction of the inward rectification in morphine-dependent rats alters the physiological properties of type III neurons. **a, b** Representative voltage responses of type III neurons from control and dependent rats, respectively. These neurons were stimulated with rectangular current steps of 350 ms duration and increases in the current level at 10 pA increments in the successive cycles. **c, d** The input resistance of the two neurons in **a** and **b** as a function of the injected current. A strong drop in input resistance at increasingly more negative current levels was associated with activation of the inward-rectifying K^+ current. Input-output curves of these neurons are shown in **e** and **f**. The rheobase of

the neuron from the control rat was ~ 85 pA, more positive than that of the neuron from the dependent animal. **g–j** The comparison of four physiological parameters of type III neurons. The resting membrane potential of type III neurons from dependent rats was more positive than that from controls (**g**). The mean input resistance at resting membrane potential (R_{rest}) was slightly increased in dependent rats (**h**) and more significantly when measured at -200 pA stimulus levels (R_{hyp}) (**i**). The rheobase of type III neurons from dependent animals was significantly reduced relative to control neurons (**j**)

under static stimulation by injection of DC pulses. We observed an increase in the dynamic excitability of type III neurons of morphine-dependent rats, i.e., a decrease of the conductance threshold of spiking for each type of input pattern delivered via the dynamic clamp. For example, the synaptic conductance threshold of firing under the first type of input (discrete EPSCs) was 17.9 ± 1.7 nS in control type III neurons and 11.3 ± 1.3 nS in dependent type III neurons ($n = 5$ vs. $n = 9$, $p = 0.01$; Fig. 2i). Also, as shown in Fig. 2a, e, the amplitudes of EPSPs are larger in dependent animals than controls. This increase in EPSP amplitude is likely a consequence of increase of input resistance. Therefore, the dynamic clamp experiments show that type III jcbNST neurons from morphine-dependent animals fire at lower conductance levels of synaptic excitation than those of control animals.

As described above, the physiological properties of type I and II neurons as measured in experiments with current step stimulation were unaffected by morphine dependence. Indeed, our dynamic clamp experiments with type I and II neurons revealed no changes in their firing threshold under the two types of simulated synaptic input in the dynamic clamp setting, e.g., for single EPSPs, the conductance threshold of dependent vs. control type II neurons was 6.3 ± 0.7 vs. 6.2 ± 0.6 nS ($n = 9$ and 7, respectively). Thus, morphine dependence induces a cell type-specific plasticity of type III neurons.

EPSP amplification is decreased in morphine dependence

Synaptic integration and EPSP-spike coupling are regulated by numerous cellular properties, including voltage-gated

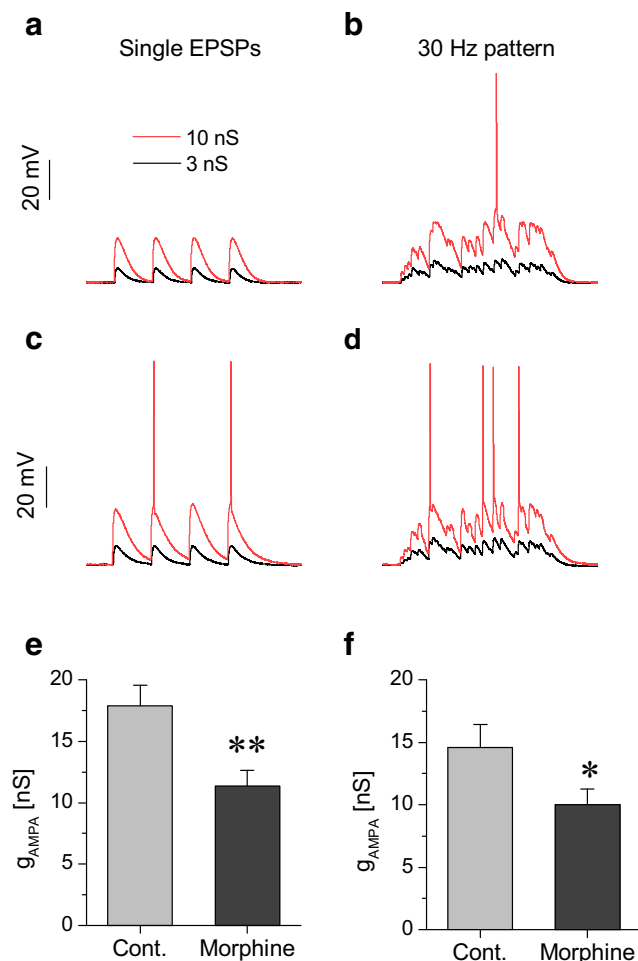


Fig. 3 Type III neurons from dependent animals fire more intensely under the action of simulated synaptic inputs with the dynamic clamp. Voltage responses of a type III neuron from a control rat (**a, b**) and dependent rat (**c, d**) are shown for two different stimulus protocols. The first protocol consisted of four EPSPs delivered at 0.25 s intervals. The black and red traces show the responses at 3 and 10 nS AMPA conductance levels, respectively. The neuron remained below spike threshold in the first example (**a**). The same neuron reached spike threshold when the second stimulus was delivered (**b**; a mixture of EPSPs and IPSPs at 30 Hz mean frequency was used here). The corresponding panels in **c** and **d** demonstrate the firing responses of the BNST neuron from the dependent rat. Here, the type III neuron exhibits more intense firing under identical stimulus strength. The graphs in **e** and **f** show the mean minimal AMPA synaptic conductance levels required to elicit firing for each protocol (threshold conductances; $n = 5$ vs. 9 for controls vs. dependent)

membrane conductances that activate near threshold. The inward-rectifying K^+ current is mostly active at resting membrane potentials and below, but the excitability of neurons also depends on the operation of depolarization-activated channels like the ones that mediate the persistent Na^+ current (I_{NaP}) (Carter et al. 2012; Crill 1996; Vervaeke et al. 2006; Wu et al. 2005). Although the amplitude of I_{NaP} is rather small compared with I_{NaT} , it has the ability to greatly influence the frequency and pattern of firing of many neurons by producing a depolarizing current in the voltage range between the resting

potential and spike threshold (Carter et al. 2012). Because of these characteristics, an effect of I_{NaP} is the amplification of EPSP (see Fig. 4) (Vervaeke et al. 2006; Wu et al. 2005). The impact of I_{NaP} on the shaping of EPSPs and synaptic integration (summation of EPSPs) has been described for several types of neurons (Carter et al. 2012; Crill 1996; Vervaeke et al. 2006; Wu et al. 2005). Therefore, our next experiments were designed to investigate possible neuroadaptive changes of EPSP kinetics that might indicate altered function of I_{NaP} in dependent animals. Here again, we utilized the dynamic clamp technique to elicit discrete EPSPs in jcBNST neurons. However, rather than increasing the strength of synaptic conductance, we gradually shifted the baseline membrane potential of the neuron. Specifically, fixed strength, 5 nS EPSCs were injected into the neuron under stimulation, and the holding current was gradually increased to reach more depolarized baseline levels (Fig. 4). In each cycle of stimulation, we elicited 10 EPSPs (separated by 0.5-s intervals) that allowed us to calculate a smooth average EPSP waveform for each membrane potential level. The voltage response of a control type III neuron under such stimulation is shown in Fig. 3a. The black trace shows the EPSPs when the neuron was held at its resting membrane potential (-71 mV). Here, EPSPs within the train were uniform and decayed rapidly. When the same neuron was held at a -54 mV membrane potential, EPSPs pushed the neuron's membrane potential near to its firing threshold, and spikes began to appear. At the same time, EPSPs that were still subthreshold became broader. This EPSP broadening was commonly observed in most jcBNST neurons, and we found no evidence of cell type-specific differences (like in the case of inward rectification, type III neurons). For each neuron under such stimulation, we calculated the average EPSP waveforms (e.g., Fig. 4b) and characterized the shape of these waveforms. In particular, the parameter most relevant to the voltage-dependent broadening of EPSPs is the half-width (HW), which was plotted against the baseline membrane potential for each experiment (Fig. 4c). We used linear fitting and calculated slope parameters that well characterized the shape of the HW vs. voltage relationship. Specifically, two sections of the curve below and above the reference voltage were fitted with linear functions, and the slopes of these lines were compared. Strong EPSP broadening manifested as a prominent jump in the slope (Fig. 4c). We found a significant loss of EPSP amplification in jcBNST neurons from morphine-dependent rats compared with control animals (Fig. 4). The change in the HW slope of jcBNST neurons from control vs. dependent animals was 19.5 ± 3.9 vs. 9.5 ± 1.9 ms/mV ($p = 0.05$), respectively. Hence, EPSP broadening near the spike threshold was approximately two times stronger in control animals than in dependent animals. It is noteworthy that the experimental conditions here differed from those in the previous dynamic clamp experiments in one important aspect. The neurons under the EPSP amplification protocol were

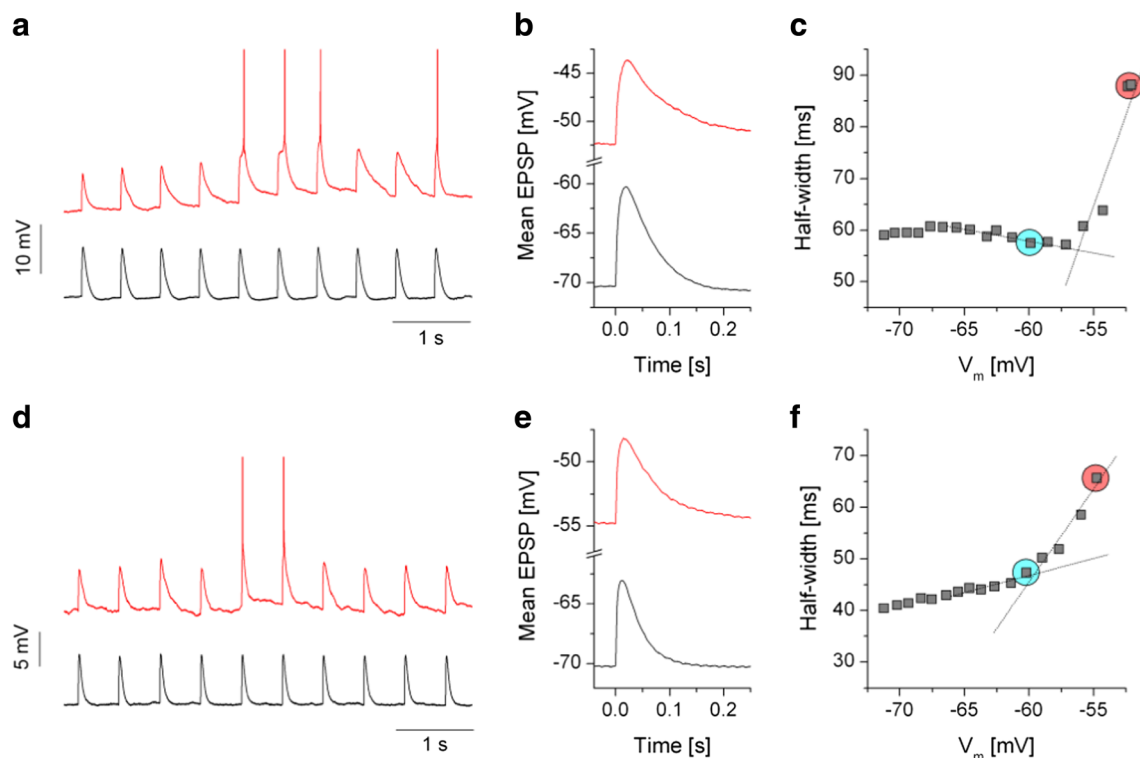


Fig. 4 Analysis of EPSP amplification using dynamic clamp and simulated excitatory synaptic inputs. **a** Voltage output of a control type III neuron in response to 10 EPSP inputs at -70 mV membrane potential (black trace) and near spike threshold (-52 mV, red trace). **b** Average EPSP waveforms calculated from the corresponding traces in **a**. The voltage dependence of the EPSP half-width is shown in **c**. The red

circle indicates the EPSP half-width near spike threshold, and the cyan circle shows the reference value at -60 mV. There was a prominent jump in the EPSP half-width as the membrane potential approached the spike threshold. A type III neuron from a dependent animal (**d**) exhibited weaker EPSP amplification than the control (**f** vs. **c**)

operating in a different voltage regime than the ones that were subjected to the dynamic excitability protocol. Specifically, the sudden jump in the HW vs. voltage function appears near -50 mV voltage levels where the inward-rectifying current is mostly deactivated. Hence, the shape of the EPSPs that were evoked at these potentials was mostly influenced by factors other than the magnitude of I_{KIR} .

Dynamic clamp simulation of the effect of I_{NaP} in jcBNST neurons

While the relationship between the degree of EPSP amplification and magnitude of I_{NaP} has been demonstrated in several brain areas and cell types (Liu and Shipley 2008b, a), the isolation of this current by means of pharmacological tools is challenging. The impact of the up- or downregulation of I_{NaP} on the functional properties of neurons has been studied by means of dynamic clamp insertion of synthetic Na_P current via dynamic clamp (Vervaeke et al. 2006). The kinetics and voltage dependence of the persistent Na^+ current is relatively simple and well-known and as such allows a realistic implementation of the synthetic Na_P current in biological neurons. To demonstrate the effect of the synthetic I_{NaP} on the EPSP amplification of jcBNST neurons, we used the experimental

approach described in the previous section (i.e., we injected trains of simulated excitatory postsynaptic currents into the neurons and varied the resting membrane potential by adding increasing levels of constant current). Concurrently, we injected the synthetic Na_P current but used a negative sign for its maximal conductance parameter. In effect, this simulated the subtraction of I_{NaP} from the biological neuron. These experiments were performed on type III neurons from control animals that show robust EPSP amplification (Fig. 5a, b). As frequently observed, the EPSP HW in such experiments began to increase steeply at membrane potentials around -55 mV. However, when the negative-conductance synthetic I_{NaP} was injected concurrently ($g_{NaP} = -1$ nS), no amplification was found. Figure 5c shows the average EPSP waveforms of a type III neuron at normal resting membrane potential and near spike threshold. Here, EPSPs were relatively sharp at both levels (compared with controls in Fig. 5a). Plotting the EPSP HW against the membrane potential resulted in a flat function (Fig. 5d). Hence, we found that EPSP amplification was strongly reduced by the subtraction of I_{NaP} in type III neurons ($n = 7$), an effect that agrees well with the partial loss of EPSP amplification in morphine-dependent rats.

By use of a combination of simulated synaptic inputs and “virtual pharmacology,” we performed another experiment to

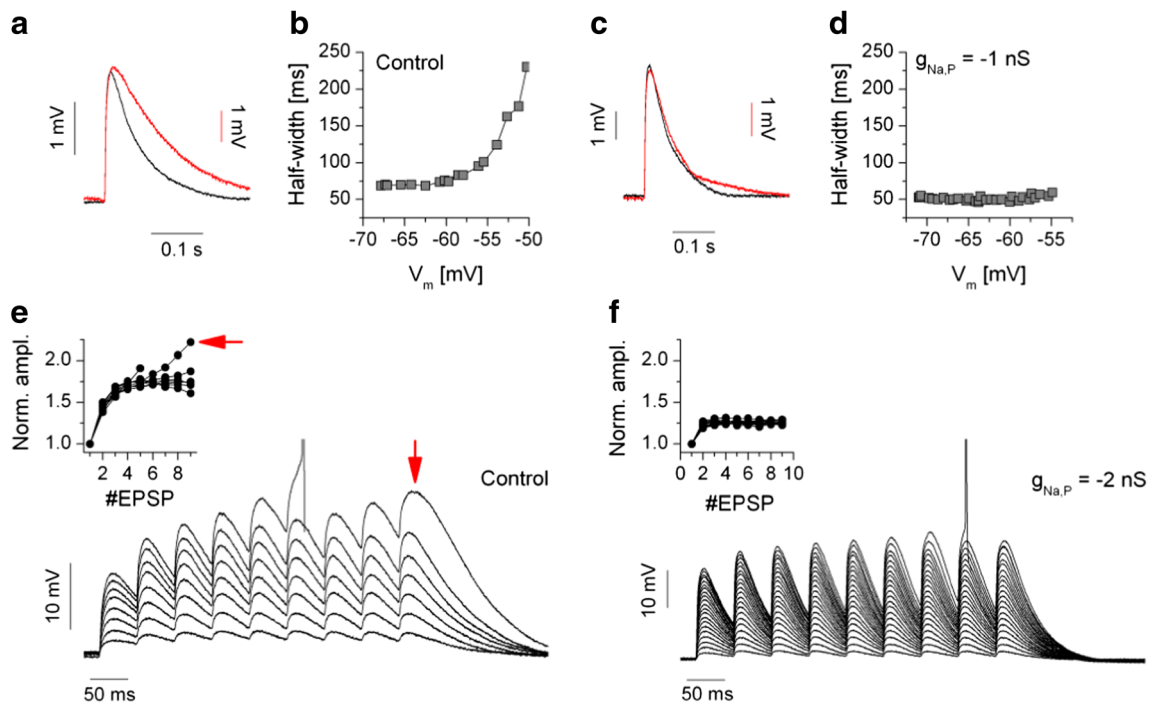


Fig. 5 Dynamic clamp subtraction of the persistent Na^+ current (I_{NaP}) reproduces the loss of EPSP amplification as observed in type III neurons of morphine-dependent animals. In these experiments, we used synthetic I_{NaP} in the dynamic clamp based on the Hodgkin-Huxley formalism. **a** Average EPSP waveforms of a control type III neuron at -70 mV and near spike threshold (red). **b** The EPSP half-width as a function of the membrane potential. This parameter increased steeply near the spike threshold. **c** When the synthetic I_{NaP} was injected at a -1 nS conductance level, EPSP amplification was lost (average EPSP

waveforms), as reflected in **d**. **e** EPSP accumulation in the same neuron was analyzed using a 20-Hz train of EPSPs. In this experiment, the strength of the synthetic AMPA conductance was gradually increased, producing an increasing amount of net excitation. The normalized EPSP amplitude (inset in **e**) increased rapidly near the spike threshold as a result of supralinear summation of EPSPs. **f** When the synthetic I_{NaP} was applied at -2 nS of the maximal conductance level, supralinear accumulation was not observed. The inset in **f** shows the normalized EPSP amplitude reflecting the lack of supralinear accumulation

test the functional effects of I_{NaP} . We analyzed how the summation (or accumulation) of EPSPs is regulated by the amount of synthetic Na_p current. Here, we used 20-Hz trains of EPSCs injected into jcBNST neurons and gradually increased synaptic conductance in the successive sweeps. The accumulation of EPSPs was evident at strong AMPA conductance levels in control type III cells (Fig. 5e). Families of normalized EPSP amplitude curves were obtained by dividing the local amplitude of each EPSP with that of the first in the train and plotting the values for each AMPA conductance level. This analysis was performed for type III neurons with and without subtracted I_{NaP} . In the latter case, normalized EPSP amplitudes were significantly reduced, with no signs of the supralinear summation of EPSPs (Fig. 5f). This analysis suggested that downregulation of the intrinsic Na_p current might impact the integrative properties of jcBNST neurons, resulting in a reduced likelihood to fire under the action of intense glutamatergic synaptic inputs.

Spontaneous synaptic transmission is unaffected by morphine dependence

Voltage-clamp recordings of jcBNST neurons were performed at -70 mV holding potentials, where spontaneous excitatory

postsynaptic currents (sEPSC) were readily observed and reached tens of pA in amplitude (normal ACSF as bath). As an initial observation, the frequency of sEPSCs in type III neurons was many times higher than that of either type I or type II cells. Typically, we observed 5–10 EPSC events per second in type III neurons, allowing a high number of samples in the duration of the recording (200–600 s). Each recording allowed us to build a smooth inter-event interval (IEI) histogram and amplitude histogram. sEPSCs that exceeded 3.5 pA in amplitude were detected using our custom algorithm. Tensecond section examples of current recordings of type III neurons from control and dependent animals are shown in Fig. 5a. For each recording, we calculated the mean sEPSC frequency and amplitude parameters and built the corresponding histograms. We found no statistically significant changes in the frequency or amplitude of sEPSC events in type III neurons when comparing the control and dependent groups. One small difference was that the sEPSC frequency across neurons of control animals spanned a wider range, and both very short and very long IEIs were more often observed compared with dependent neurons. This effect produced a slightly more slanted cumulative IEI histogram in the pooled dataset (Fig. 6c). We note that the prior application of 100 nM

tetrodotoxin (TTX) in a few test experiments did not change the frequency or amplitude of sEPSCs, indicating that they were, in fact, miniature events.

Discussion

The BNST is a key site of neuroadaptations of behavioral significance induced by drugs of abuse (Aston-Jones et al. 1999; Buffalari and See 2011; Dumont et al. 2005; Dumont et al. 2008; Epping-Jordan et al. 1998; Francesconi et al. 2009; Francesconi et al. 2009; Harris and Aston-Jones 2007; Kash et al. 2009; Krawczyk et al. 2011; Wills et al. 2012). A growing body of evidence supports that drugs of abuse in addition to affecting synaptic dynamics can also induce plastic changes of the intrinsic membrane properties, which have significant implications for the integrative properties of neurons (Kourrich et al. 2015). Synaptic changes in response to drugs of abuse have been previously described in the BNST (Dumont et al. 2005; Dumont et al. 2008; Egli et al. 2005; Krawczyk et al. 2011; Wills et al. 2012). Our previous work also showed that the jcBNST undergoes long-term changes of its intrinsic properties in animals with a history of dependence on drugs or alcohol during protracted abstinence (Francesconi et al. 2009; Szucs et al. 2012). For instance, a history of dependent self-administration of heroin, cocaine, and alcohol and chronic intracerebroventricular administration of the stress peptide corticotropin-releasing factor lead to the progressive and persistent impairment of a form of activity-dependent plasticity of the intrinsic excitability of all three neuronal cell types in the jcBNST, which depends on altered dynamic regulation of the α -dendrotoxin (α -DTX)-sensitive or D-type K^+ current (I_D) (Francesconi et al. 2009). Additionally, alcohol dependence is associated with reduced excitability of the three jcBNST neuronal cell types during protracted abstinence (Szucs et al. 2012). Here, we show that a history of morphine dependence induces both cell type-specific and common changes in the intrinsic and integrative properties of jcBNST neurons during protracted withdrawal. In particular, unlike previous studies in which we observed changes common to all three jcBNST neuronal types (Francesconi et al. 2009; Szucs et al. 2012), here, we report that opioid dependence reduces the rheobase of type III neurons when stimulated with DC pulses as well as increases their excitability under simulated synaptic bombardment with the dynamic clamp. This increase in the excitability of jcBNST type III neurons was associated with an increase in the input resistance of the cell and with a shift of the resting membrane potential toward depolarization. These changes in the membrane properties suggest a reduction of the inward-rectifying K^+ current (I_{KIR}), which characterizes this jcBNST cell type. Importantly, the degree of increase of membrane resistance was greater at -200 pA current level than at resting membrane

potential, suggesting a key role of the K_{ir} current mediating this effect. Additionally, we observed a reduction of EPSP amplification in all three neuronal cell types in the jcBNST, suggesting a reduction of the persistent Na current (I_{NaP}).

The I_{KIR} , which mediates the inward rectification that is present in type III jcBNST neurons, is responsible for the hyperpolarized resting membrane potential and reduced spontaneous electrical activity of the neurons that express it (Hammack et al. 2007; Uchimura et al. 1989). The I_{KIR} is also a major determinant of the input resistance at voltages near resting membrane potential and below. I_{KIR} stabilizes the membrane close to K^+ equilibrium potential, opposing excitatory inputs. Thus, changes in the magnitude of this conductance could affect responses to excitatory inputs in some cell types, for instance, in nucleus accumbens medium spiny neurons (John and Manchanda 2011; Kourrich et al. 2015; Wilson and Kawaguchi 1996). Cell type-selective increases in the I_{KIR} have been shown in the superficial dorsal horn leading to persistent alterations in pain sensitivity (Li and Baccei 2014). I_{NaP} is activated at more negative potentials (approximately 10 mV below the spike threshold) than the spike-generating transient Na^+ current (I_{NaT}) (Crill 1996). Also importantly, I_{NaP} is activated rapidly, like the spike-generating transient Na^+ current (I_{NaT}); however, unlike I_{NaT} , I_{NaP} is slowly inactivating (i.e., “persistent”) (Crill 1996). The slow inactivation of I_{NaP} is responsible for the amplification of the EPSP. Although I_{NaP} is rather small compared with I_{NaT} , it has the ability to greatly influence the frequency and pattern of firing of many neurons by producing a depolarizing current in the voltage range between the resting potential and spike threshold (Carter et al. 2012). Because of these characteristics, an effect of I_{NaP} is the amplification of EPSP (see Fig. 4) (Vervaeke et al. 2006; Wu et al. 2005).

The membrane depolarization and the increase of input resistance, caused by the reduction of both I_{KIR} and I_{NaP} in dependent rats, suggest that the synaptic responses of these neurons might be stronger in rats with a history of opioid dependence than in control rats. The present dynamic clamp experiments support this hypothesis (Fig. 3). Hence, the present findings show that neuroadaptive alterations of intrinsic membrane properties can result in the differential regulation of firing responses of type III jcBNST neurons. In a recent computational study, we explored this hypothesis by exposing 7-conductance model neurons to both static current step stimulation and simulated synaptic bombardment (Szucs and Huerta 2015). We found that changes in a specific voltage-gated membrane current, such as the inward-rectifying K^+ current, can regulate the postsynaptic firing responses more effectively than the static responses under the current step stimulation. This notion is consistent with our present observations. Additionally, our prior study on jcBNST neurons from rats with a history of alcohol dependence demonstrated similar differences in the regulation of static vs. dynamic

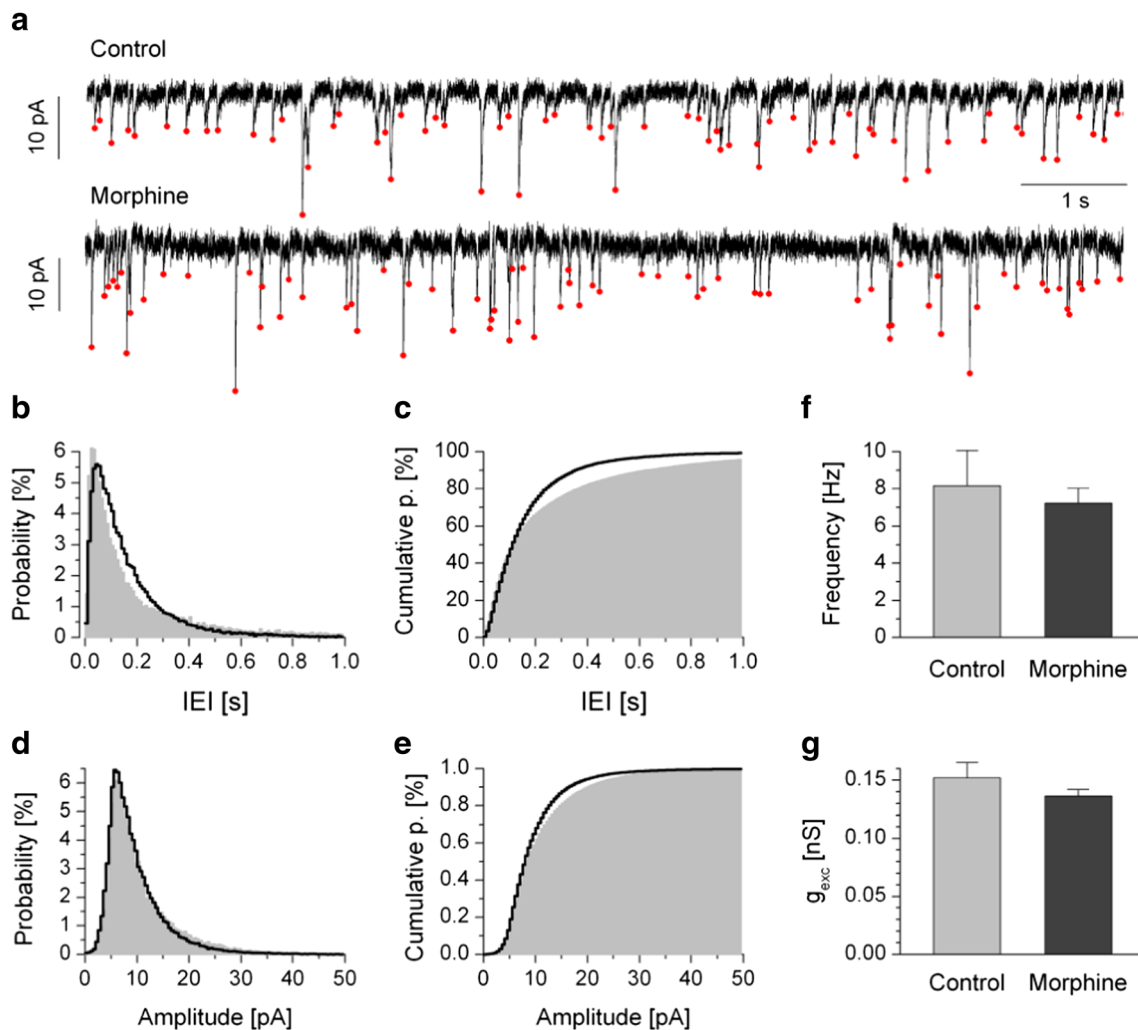


Fig. 6 The average frequencies and amplitudes of spontaneous EPSCs of type III neurons did not significantly differ from controls. **a** Representative traces of transmembrane current (10 s sections) recorded from type III neurons of control and dependent animals ($V_{hold} = -70$ mV). Average probability distributions and cumulative probabilities are shown in **b** and **c**, respectively (gray areas for controls, $n = 11$; black lines for dependent, $n = 17$). The relative count of both short

(< 0.1 s) and long (> 0.5 s) IEIs was slightly reduced in cells of dependent animals compared with controls. This produced a more steeply rising cumulative IEI histogram in **c**. sEPSC amplitudes were analyzed in a similar manner (**d** and **e**) using histograms in the 0–50 pA range. The mean sEPSC frequency and amplitude from the pooled data are shown in **f** and **g**, respectively

excitability, supporting the importance of studying neuroadaptive changes induced by drugs and alcohol abuse with dynamic clamp protocols designed to simulate *in vivo* conditions (Szucs et al. 2012). Here, firing responses of jcBNST neurons under simulated synaptic bombardment were strongly reduced by the alcohol-dependent upregulation of their D-type K currents. At the same time, measures of static excitability were not significantly altered.

The transition to addiction is believed to involve the progressive failure of normal homeostatic processes of reward and stress brain circuits, leading to pathophysiology through the failure to return within the normal homeostatic range and emergence of an “allostatic state” (Koob and Le Moal 2001). Allostasis is a break with normal homeostatic processes that allows apparent “stability with change” but results in a cost to

the system and a reduction of the capacity to meet the demands from external forces because of decreased margins for further adjustments (Koob and Le Moal 2001). The present results of increased excitability and activity of type III jcBNST neurons in brain slices from rats with a history of opioid dependence suggest that changes in the intrinsic properties of type III jcBNST neurons can represent the allostatic dysregulation of potential functional consequences to circuit functioning. Neuronal activity is stabilized by a complex array of homeostatic mechanisms that are aimed at adjusting excitability to maintain a reasonably constant level of activity through a negative feedback system (Turrigiano 2012). From an allostatic perspective, it can be hypothesized that the present changes in the intrinsic properties of type III neurons may be a response to reduced activity of presynaptic inputs, aimed

at homeostatically adjusting overall activity in the circuit. Presynaptic inputs to these neurons were unaffected by a history of opioid dependence. However, the level of activity to which these neurons are subjected *in vivo* is not reflected in the *in vitro* setting, in which neurons in brain slices are mostly quiescent. It is also possible that the increased excitability could be maladaptive and result in an imbalance between inhibition and excitation of a circuit, which could lead to pathologically enhanced or reduced circuit excitability, amplification, or silencing of inputs to a circuit and changes in the precision or the degree to which neurons in a circuit become synchronized.

At the circuit level, the unique connectivity of the jcBNST suggests a key role in integrating cortical and amygdala inputs and provides feed-forward inhibition to the CeA (Francesconi et al. 2009). In particular, the jcBNST has direct projections to the medial part of the central nucleus of the amygdala (CeAm), like other cell groups of the anterolateral BNST (Dong et al., 2000). The contribution of the individual cell type to the projections of the jcBNST is currently unknown. However, if type III neurons contribute to the inhibitory projections to the CeA, the present results would be consistent with an increased inhibitory drive to the CeA. Conversely, the downregulation of the I_{NaP} in neurons other than the type III, in which I_{KIR} downregulation is expected to be dominant, may result in decreased excitability and reduced precision in the circuit in which they are active due to loss of EPSP amplification (Fricker and Miles 2000). Similarly, divergent effects have been described in other nuclei regulating the output of the amygdala. For instance, fear conditioning induces distinct forms of plasticity in neuronal populations of the lateral part of the central nucleus of the amygdala (CEAL), which also provides inhibitory inputs to the CeAm (Ciocchi et al. 2010; Duvarci et al. 2011; Haubensak et al. 2010). The CeA is an autonomic-projecting region, which has been suggested to constitute a “visceromotor striatum” (Swanson and Petrovich 1998). Since both the jcBNST (Dong et al., 2000) and the CeA receive nociceptive information (Bernard and Besson 1990; Bernard et al. 1990), changes in the excitability of the jcBNST in rats with history of morphine dependence are likely to contribute to the hyperalgesia observed in these rats. Allostatic adaptation of circuits involving the BNST and the CeA is expected to affect descending regulation of the periaqueductal gray matter (PAG) in the brainstem and its role in integrating nociceptive inputs arriving from the ascending pain pathways (Elman et al. 2013; Hayes and Northoff 2012).

Conclusions

The identification of the cellular and molecular consequences of opioid dependence is critical to the development of new and more effective therapeutic strategies for opioid dependence.

We previously observed that histories of drug and alcohol abuse modify the intrinsic properties of jcBNST neurons leading to changes in excitability and capacity for plasticity of their intrinsic excitability (Francesconi et al. 2009; Szucs et al. 2012). In the present study, we found that a history of morphine dependence augments both the static and dynamic excitability of a specific jcBNST cell type during opioid withdrawal. By altering the activity of extended amygdala circuits where they are embedded, changes in the integration properties of jcBNST neurons may contribute to the emotional dysregulation associated with drug dependence and withdrawal.

Acknowledgements This work was supported by National Institutes of Health grants DA031566, DA043268 and the Hungarian National Brain Research Program grant KTIA_NAP_13-2014-0018.

References

- Angst MS, Clark JD (2006) Opioid-induced hyperalgesia: a qualitative systematic review. *Anesthesiology* 104:570–587
- Aston-Jones G, Delfs JM, Druhan J, Zhu Y (1999) The bed nucleus of the stria terminalis. A target site for noradrenergic actions in opiate withdrawal. *Ann N Y Acad Sci* 877:486–498
- Aston-Jones G, Harris GC (2004) Brain substrates for increased drug seeking during protracted withdrawal. *Neuropharmacology* 47(Suppl 1):167–179
- Bernard JF, Besson JM (1990) The spino(trigemino)pontoamygdaloid pathway: electrophysiological evidence for an involvement in pain processes. *J Neurophysiol* 63:473–490
- Bernard JF, Huang GF, Besson JM (1990) Effect of noxious somesthetic stimulation on the activity of neurons of the nucleus centralis of the amygdala. *Brain Res* 523:347–350
- Buffalari DM, See RE (2011) Inactivation of the bed nucleus of the stria terminalis in an animal model of relapse: effects on conditioned cue-induced reinstatement and its enhancement by yohimbine. *Psychopharmacology* 213:19–27
- Carrera MR, Schulteis G, Koob GF (1999) Heroin self-administration in dependent Wistar rats: increased sensitivity to naloxone. *Psychopharmacology* 144:111–120
- Carter BC, Giessel AJ, Sabatini BL, Bean BP (2012) Transient sodium current at subthreshold voltages: activation by EPSP waveforms. *Neuron* 75:1081–1093
- Ciocchi S, Herry C, Grenier F, Wolff SB, Letzkus JJ, Vlachos I, Ehrlich I, Sprengel R, Deisseroth K, Stadler MB, Müller C, Luthi A (2010) Encoding of conditioned fear in central amygdala inhibitory circuits. *Nature* 468:277–282
- Crill WE (1996) Persistent sodium current in mammalian central neurons. *Annu Rev Physiol* 58:349–362
- De Campo DM, Fudge JL (2013) Amygdala projections to the lateral bed nucleus of the stria terminalis in the macaque: comparison with ventral striatal afferents. *J Comp Neurol* 521:3191–3216
- Diana M, Muntoni AL, Pistis M, Melis M, Gessa GL (1999) Lasting reduction in mesolimbic dopamine neuronal activity after morphine withdrawal. *Eur J Neurosci* 11:1037–1041
- Dong H, Petrovich GD, Swanson LW (2000) Organization of projections from the juxtacapsular nucleus of the BST: a PHAL study in the rat. *Brain Res* 859:1–14
- Dong HW, Petrovich GD, Swanson LW (2001) Topography of projections from amygdala to bed nuclei of the stria terminalis. *Brain Res Brain Res Rev* 38:192–246

- Dumont EC, Mark GP, Mader S, Williams JT (2005) Self-administration enhances excitatory synaptic transmission in the bed nucleus of the stria terminalis. *Nat Neurosci* 8:413–414
- Dumont EC, Rycroft BK, Maiz J, Williams JT (2008) Morphine produces circuit-specific neuroplasticity in the bed nucleus of the stria terminalis. *Neuroscience* 153:232–239
- Duvarci S, Popa D, Pare D (2011) Central amygdala activity during fear conditioning. *J Neurosci* 31:289–294
- Edwards S, Vendruscolo LF, Schlosburg JE, Misra KK, Wee S, Park PE, Schulteis G, Koob GF (2012) Development of mechanical hypersensitivity in rats during heroin and ethanol dependence: alleviation by CRF(1) receptor antagonism. *Neuropharmacology* 62:1142–1151
- Egli RE, Kash TL, Choo K, Savchenko V, Matthews RT, Blakely RD, Winder DG (2005) Norepinephrine modulates glutamatergic transmission in the bed nucleus of the stria terminalis. *Neuropsychopharmacology* 30:657–668
- Elman I, Borsook D, Volkow ND (2013) Pain and suicidality: insights from reward and addiction neuroscience. *Prog Neurobiol* 109:1–27
- Epping-Jordan MP, Markou A, Koob GF (1998) The dopamine D-1 receptor antagonist SCH 23390 injected into the dorsolateral bed nucleus of the stria terminalis decreased cocaine reinforcement in the rat. *Brain Res* 784:105–115
- Francesconi W, Berton F, Koob GF, Sanna PP (2009) Intrinsic neuronal plasticity in the juxtacapsular nucleus of the bed nuclei of the stria terminalis (jcBNST). *Prog Neuro-Psychopharmacol Biol Psychiatry* 33:1347–1355
- Francesconi W, Berton F, Repunte-Canonigo V, Hagihara K, Thurbon D, Lekic D, Specio SE, Greenwell TN, Chen SA, Rice KC, Richardson HN, O'Dell LE, Zorrilla EP, Morales M, Koob GF, Sanna PP (2009) Protracted withdrawal from alcohol and drugs of abuse impairs long-term potentiation of intrinsic excitability in the juxtacapsular bed nucleus of the stria terminalis. *J Neurosci* 29:5389–5401
- Frenk SM, Porter KS, Paulozzi LJ (2015) Prescription opioid analgesic use among adults: United States, 1999–2012. NCHS Data Brief: 1–8
- Fricke D, Miles R (2000) EPSP amplification and the precision of spike timing in hippocampal neurons. *Neuron* 28:559–569
- Gold LH, Stinus L, Inturrisi CE, Koob GF (1994) Prolonged tolerance, dependence and abstinence following subcutaneous morphine pellet implantation in the rat. *Eur J Pharmacol* 253:45–51
- Goldner EM, Lusted A, Roerecke M, Rehm J, Fischer B (2014) Prevalence of axis-I psychiatric (with focus on depression and anxiety) disorder and symptomatology among non-medical prescription opioid users in substance use treatment: systematic review and meta-analyses. *Addict Behav* 39:520–531
- Hammack SE, Mania I, Rainnie DG (2007) Differential expression of intrinsic membrane currents in defined cell types of the anterolateral bed nucleus of the stria terminalis. *J Neurophysiol* 98:638–656
- Harris GC, Aston-Jones G (2007) Activation in extended amygdala corresponds to altered hedonic processing during protracted morphine withdrawal. *Behav Brain Res* 176:251–258
- Haubensak W, Kunwar PS, Cai H, Ciochi S, Wall NR, Ponnusamy R, Biag J, Dong HW, Deisseroth K, Callaway EM, Fanselow MS, Luthi A, Anderson DJ (2010) Genetic dissection of an amygdala microcircuit that gates conditioned fear. *Nature* 468:270–276
- Hayes DJ, Northoff G (2012) Common brain activations for painful and non-painful aversive stimuli. *BMC Neurosci* 13:60
- Hazra R, Guo JD, Ryan SJ, Jasnow AM, Dabrowska J, Rainnie DG (2011) A transcriptomic analysis of type I–III neurons in the bed nucleus of the stria terminalis. *Mol Cell Neurosci* 46:699–709
- John J, Manchanda R (2011) Modulation of synaptic potentials and cell excitability by dendritic KIR and KAs channels in nucleus accumbens medium spiny neurons: a computational study. *J Biosci* 36:309–328
- Kash TL, Baucum AJ 2nd, Conrad KL, Colbran RJ, Winder DG (2009) Alcohol exposure alters NMDAR function in the bed nucleus of the stria terminalis. *Neuropsychopharmacology* 34:2420–2429
- Koob GF, LeMoal M (2001) Drug addiction, dysregulation of reward, and allostasis. *Neuropsychopharmacology* 24:97–129
- Koob GF, Volkow ND (2010) Neurocircuitry of addiction. *Neuropsychopharmacology* 35:217–238
- Kourrich S, Calu DJ, Bonci A (2015) Intrinsic plasticity: an emerging player in addiction. *Nat Rev Neurosci* 16:173–184
- Krawczyk M, Sharma R, Mason X, Debacker J, Jones AA, Dumont EC (2011) A switch in the neuromodulatory effects of dopamine in the oval bed nucleus of the stria terminalis associated with cocaine self-administration in rats. *J Neurosci* 31:8928–8935
- Larriva-Sahd J (2004) Juxtacapsular nucleus of the stria terminalis of the adult rat: extrinsic inputs, cell types, and neuronal modules: a combined Golgi and electron microscopic study. *J Comp Neurol* 475:220–237
- Li J, Baccei ML (2014) Neonatal tissue injury reduces the intrinsic excitability of adult mouse superficial dorsal horn neurons. *Neuroscience* 256:392–402
- Liu S, Shipley MT (2008a) Intrinsic conductances actively shape excitatory and inhibitory postsynaptic responses in olfactory bulb external tufted cells. *J Neurosci* 28:10311–10322
- Liu S, Shipley MT (2008b) Multiple conductances cooperatively regulate spontaneous bursting in mouse olfactory bulb external tufted cells. *J Neurosci* 28:1625–1639
- McDonald AJ, Shammah-Lagnado SJ, Shi C, Davis M (1999) Cortical afferents to the extended amygdala. *Ann N Y Acad Sci* 877:309–338
- Nowotny T, Szücs A, Pinto RD, Selverston AI (2006) StpC: a modern dynamic clamp. *J Neurosci Methods* 158:287–299
- Ren ZY, Shi J, Epstein DH, Wang J, Lu L (2009) Abnormal pain response in pain-sensitive opiate addicts after prolonged abstinence predicts increased drug craving. *Psychopharmacology* 204:423–429
- SAMHSA (2013) Results from the 2012 National Survey on Drug Use and Health: Summary of National Findings, NSDUH Series H-46, HHS Publication No. (SMA) 13-4795. Rockville, MD: Substance Abuse and Mental Health Services Administration, 2013. <http://www.samhsa.gov/data/NSDUH/2012SummNatFindDetTables/Index.aspx>
- Shammah-Lagnado SJ, Santiago AC (1999) Projections of the amygdalopiriform transition area (APir). A PHA-L study in the rat. *Ann N Y Acad Sci* 877:655–660
- Shurman J, Koob GF, Gutstein HB (2010) Opioids, pain, the brain, and hyperkatifeia: a framework for the rational use of opioids for pain. *Pain Med* 11:1092–1098
- Silberman Y, Winder DG (2013) Emerging role for corticotropin releasing factor signaling in the bed nucleus of the stria terminalis at the intersection of stress and reward. *Front Psychiatry* 4:42
- Simonnet G, Rivat C (2003) Opioid-induced hyperalgesia: abnormal or normal pain? *Neuroreport* 14:1–7
- Stamatakis AM, Sparta DR, Jennings JH, McElligott ZA, Decot H, Stuber GD (2014) Amygdala and bed nucleus of the stria terminalis circuitry: implications for addiction-related behaviors. *Neuropharmacology* 76(Pt B):320–328
- Stinus L, Caille S, Koob GF (2000) Opiate withdrawal-induced place aversion lasts for up to 16 weeks. *Psychopharmacology* 149:115–120
- Swanson LW, Petrovich GD (1998) What is the amygdala? *Trends Neurosci* 21:323–331
- Szucs A, Berton F, Nowotny T, Sanna P, Francesconi W (2010) Consistency and diversity of spike dynamics in the neurons of bed nucleus of stria terminalis of the rat: a dynamic clamp study. *PLoS One* 5:e11920
- Szucs A, Berton F, Sanna PP, Francesconi W (2012) Excitability of jcBNST neurons is reduced in alcohol-dependent animals during protracted alcohol withdrawal. *PLoS One* 7:e42313
- Szucs A, Huerta R (2015) Differential effects of static and dynamic inputs on neuronal excitability. *J Neurophysiol* 113:232–243

- Tran L, Schulkin J, Greenwood-Van Meerveld B (2014) Importance of CRF receptor-mediated mechanisms of the bed nucleus of the stria terminalis in the processing of anxiety and pain. *Neuropsychopharmacology* 39:2633–2645
- Turrigiano G (2012) Homeostatic synaptic plasticity: local and global mechanisms for stabilizing neuronal function. *Cold Spring Harb Perspect Biol* 4:a005736
- Uchimura N, Cherubini E, North RA (1989) Inward rectification in rat nucleus accumbens neurons. *J Neurophysiol* 62:1280–1286
- Vervaeke K, Hu H, Graham LJ, Storm JF (2006) Contrasting effects of the persistent Na⁺ current on neuronal excitability and spike timing. *Neuron* 49:257–270
- Wills TA, Klug JR, Silberman Y, Baucum AJ, Weitlauf C, Colbran RJ, Delpire E, Winder DG (2012) GluN2B subunit deletion reveals key role in acute and chronic ethanol sensitivity of glutamate synapses in bed nucleus of the stria terminalis. *Proc Natl Acad Sci U S A*
- Wilson CJ, Kawaguchi Y (1996) The origins of two-state spontaneous membrane potential fluctuations of neostriatal spiny neurons. *J Neurosci* 16:2397–2410
- Wu N, Enomoto A, Tanaka S, Hsiao CF, Nykamp DQ, Izhikevich E, Chandler SH (2005) Persistent sodium currents in mesencephalic V neurons participate in burst generation and control of membrane excitability. *J Neurophysiol* 93:2710–2722
- Yoburn BC, Chen J, Huang T, Inturrisi CE (1985) Pharmacokinetics and pharmacodynamics of subcutaneous morphine. *J Pharmacol Exp Ther* 235:282–286